

Anthesis synchronization and floral morphology determine diurnal patterns of ragweed pollen dispersal

Michael D. Martin^a, Marcelo Chamecki^b, Grace S. Brush^{a,*}

^a Department of Geography and Environmental Engineering, Johns Hopkins University, 3400 North Charles Street, Baltimore, MD 21218, USA

^b Department of Meteorology, Pennsylvania State University, 506 Walker Building, University Park, PA 16802, USA

ARTICLE INFO

Article history:

Received 21 September 2009

Received in revised form 1 June 2010

Accepted 1 June 2010

Keywords:

Ambrosia artemisiifolia

Anthesis

Dehiscence

Dispersal

Diurnal

Pistillodium

Pollen

Ragweed

ABSTRACT

Diurnal cycles of pollen dispersal are an important aspect of gene flow between wind-pollinated plants. Previous attempts to correlate these cycles with variation in meteorological factors have had little success. In *Ambrosia artemisiifolia* (common ragweed) and other species which produce aeroallergenic pollen, these cycles also present a major burden to public health. In a large field dominated by *A. artemisiifolia*, we collected measurements of low-atmosphere pollen concentration and pollen release from individual *A. artemisiifolia* flowers. We then constructed a relatively simple model that relates early morning variations in relative humidity to the probability distribution of anther dehiscence initiation timing and incorporates quantitative data on the progression of diurnal pollen release from individual male flowers. The model successfully predicts normalized pollen concentration above the field. We suggest that the extension of a tiny floral organ unique to this genus and some closely related taxa explains a ubiquitous, but previously overlooked, large-scale feature in patterns of *A. artemisiifolia* pollen dispersal. Our study shows that pollen release at the flower scale is a physiological characteristic that is intrinsically bimodal, but highly asynchronous anther rupture caused by variations in relative humidity sometimes obscures this effect and determines the overall pattern of pollen release at the scale of the entire field. We suggest that future attempts to predict diurnal pollen dispersal cycles should consider direct observations of species-specific floral development and morphology.

© 2010 Elsevier B.V. All rights reserved.

1. Introduction

In addition to year-to-year and seasonal variation, anemophilous (wind-pollinated) plants often exhibit diurnal cycles of pollen dispersal that are closely linked to meteorological factors (Jones, 1952; Ogden and Hayes, 1969; von Wahl and Puls, 1989; Norris-Hill, 1999; Jones and Harrison, 2004; Laursen et al., 2007; van Hout et al., 2008). An understanding of the relationship between these diurnal cycles and local meteorology is important for predicting and controlling haploid gene flow from transgenic populations (McCartney and Lacey, 1991; Dow and Ashley, 1998; Luna et al., 2001; Beckie and Hall, 2008). When the species in question produces pollen that is a known aeroallergen, a thorough understanding of diurnal pollen dispersal should benefit forecasts of airborne pollen delivery to local and long-distance human population centers by better differentiating the relative contributions to total pollen load of different source populations across a geographic region (Saar et al., 2000; Šikoparija et al., 2006, 2009; Cecchi et al., 2007; Stach et al., 2007). In invasive species,

haploid gene flow can facilitate the increase in genetic diversity often associated with populations in the novel range (Genton et al., 2005; Ellstrand and Schierenbeck, 2000).

A complete model of haploid gene flow (cross-pollination) between individuals of an anemophilous species must accurately account for pollen release, atmospheric transport and deposition, changes in pollen viability due to environmental exposure (Bassani et al., 1994) and fertilization success (Aylor et al., 2003). Adequate models exist for transport and deposition of pollen grains in atmospheric turbulence, but models of this sort rely on measures of canopy-level pollen concentration as input (e.g. Arritt et al., 2007; Chamecki et al., 2009). More robust models capable of predicting pollen transport in fully theoretical scenarios would also need to account for pollen release. Due to the active and species-specific nature of pollen release mechanisms, the most difficult component of a complete model of this sort is characterizing the pollen release phase. Because of these complexities, initial pollen release remains an underexplored area of study.

The circadian nature of anemophilous pollen dispersal cycles suggests their strong dependence on environmental cues, but accurate and consistent predictions of these cycles with the usual approach of directly relating meteorological conditions with airborne pollen concentrations have so far been elusive (Holmes

* Corresponding author. Tel.: +1 410 516 7107; fax: +1 410 516 8996.
E-mail address: gbrush@jhu.edu (G.S. Brush).

and Bassett, 1963; Solomon, 1984; McCartney and Lacey, 1991; Alba et al., 2000; Galán et al., 2000; Munoz et al., 2000; Barnes et al., 2001a,b; Weber, 2003; Crimi et al., 2004; Laursen et al., 2007). Problematically, these studies often take place at a distance from the pollen source so that the true nature of the relationship between meteorological conditions at the source location and pollen release and initial entrainment into the atmosphere remain obscured by stochastic effects of atmospheric transport and mixing. For this reason, despite general agreement on the diurnal cycle of release/dispersion from a particular species, frequent exceptions exist that render predictions highly unreliable (Weber, 2003).

Various measurements of gross meteorological conditions are often reported alongside measurements of airborne pollen concentration with a suggested causal relationship. However, in very few cases are these meteorological conditions used in a simulation to demonstrate causality by modelling diurnal variations in atmospheric pollen concentration. Laursen et al. (2007) developed a multiple regression model relating wind speed and temperature with hourly airborne *Artemisia tridentata* pollen concentrations that achieved an agreement with $r^2=0.77$ over one 24-h period. However, they offered little physical interpretation of this best-fit model generated using the variables showing greatest correlation with pollen concentration. This lack of direct causality may be why the model was unsuccessful for the two other 24-h sampling intervals considered.

Variability in the characteristic anther dehiscence (anther rupture, anthesis) time across plant species (Jones, 1952) suggests the importance of relationships between species-specific floral anatomy/physiology and environmental factors. Indeed, the general lack of success in correlating anemophilous pollen dispersal with gross meteorological conditions may, in part, be due to the dearth of knowledge on how and which environmental cues influence flower opening and anther dehiscence in individual species. Temperature has been found to be a principal factor in floral motion in many taxa (Percival, 1950; Stirton, 1983; Tanaka et al., 1987; von Hase et al., 2006). Along with relative humidity, it is the meteorological factor best correlated with variations in airborne diurnal pollen load (Galán et al., 2000; Weber, 2003; Crimi et al., 2004). Changes in relative humidity and the vapor pressure deficit often affect pollen release timing due to the strong influence of local relative humidity on the rupture of anther cell walls (Jones, 1952; Keijzer, 1983, 1999; Jarosz et al., 2005). Physiological changes in the anther and surrounding tissues, including osmotic swelling and coordinated dehydration, also play a critical role (Keijzer, 1999).

Ambrosia artemisiifolia (common ragweed) is one species in which the relation between environmental cues and anther dehiscence has been studied in detail. Bianchi et al. (1959) observed pollen release and anther dehiscence in relation to various environmental factors and showed that relative humidity and temperature were the principal determinants of mean dehiscence time in staminate florets. Worldwide, there are about 40 species in the genus *Ambrosia*, although by far the most successful species is *A. artemisiifolia*, a wind-pollinated, herbaceous plant that grows in sunny, disturbed soils such as riparian areas, along roadsides, and in agricultural fields (Payne, 1963). *A. artemisiifolia* is self-incompatible (Friedman and Barrett, 2008) and monoecious, with male and female flowers spatially separated on the same plant. It is also a globally invasive species that has spread from its native North America to Europe (Dahl et al., 1999; Rybnček and Jäger, 2001; Laaidi et al., 2003; Tamarcaz et al., 2005; Chauvel et al., 2006; Kiss and Beres, 2006), Australia (Bass et al., 2000), China (Wang et al., 1985), Japan (Sugaya et al., 1997), Russia (Ostroumov, 1971), Israel (Waisel et al., 2008), and beyond – just over the last 100 years. Anti-*Ambrosia* battles rage worldwide and include various strategies for eradication, containment, and prevention (Tamarcaz et al., 2005).

The extraordinarily allergenic pollen of *A. artemisiifolia* is often the main cause of allergic rhinitis in humans (Comtois and Gagnon, 1988; Roitt et al., 1996). More than 10% of the U.S. population is sensitive to *Ambrosia* pollen (Gergen et al., 1987), and rates of sensitization are rapidly increasing around the world, representing a significant cost to public health. In Hungary, the recent invasion of *A. artemisiifolia* has resulted over the past 40 years in an increase in allergic asthma by a factor of four (Makra et al., 2004). There, *A. artemisiifolia* pollen represents about half the total airborne pollen load. At present, individual plants may produce up to 3 billion pollen grains per season (Fumanal et al., 2007), but pollen production and allergenicity are expected to increase with rising levels of atmospheric CO₂ (Ziska and Caulfield, 2000; Singer et al., 2005; Stinson and Bazzaz, 2006).

In the present work, we argue that patterns of variability in pollen concentration above a large field of flowering *A. artemisiifolia* plants are best explained by both the characteristic behavior of individual male flowers during pollen release and the degree to which all the flowers in the field initiate the pollen diurnal release process in synchrony. We report the results of a model that combines data collected from videos of pollen release from individual flowers with relationships derived from previously published measurements of anther dehiscence versus local relative humidity. The model agrees well with measurements of airborne pollen concentration, which suggests that we have identified the major factors that determine some characteristics of allergenic pollen dispersal from populations of this invasive weed.

2. Materials and methods

2.1. Field experiment and data analysis

Meteorological and palynological data were collected during September and October 2006 in a fallow agricultural field invaded by *A. artemisiifolia* in Upper Marlboro, Maryland, USA (38°52'42"N 76°46'42"W). The 6.0-ha field was left undisturbed throughout 2006, after being harvested and mowed the previous year. See Martin et al. (2009) for a detailed account of field measurement methods and data analysis. Note that measurements on 29 September and 2 October had been taken after the field had been heavily modified by removing most of the *A. artemisiifolia* plants for experimental purposes (see Chamecki et al., 2009). No other populations of any *Ambrosia* species were located within 1.5 km of the field.

For most sampling days, Rotorod pollen samplers (Multidata) were vertically mounted along a 6.0-m pole at 2.0, 2.4, 2.9, 4.0, 5.0, and 6.0 m above ground level. Near the conclusion of the field experiment, the pollen samplers were mounted on poles distributed across the field. In this arrangement, measurements were collected at 2.0, 2.5, and 3.0 m above ground level. Sampler rotation rates were calibrated with a high frequency strobe light before beginning the experiment. Under a light microscope at 100–400× magnification, *Ambrosia* pollen grains were counted in lengthwise sweeps of the Rotorod collecting rods. These counts were used to calculate hourly averages of airborne pollen concentration according to Rotorod documentation. Pollen captured on the Rotorod samplers belonged overwhelmingly to genus *Ambrosia*. Contamination of the samples by pollen of other genera was extremely low, further supporting the assumption that pollen considered in this study originated in the source field. Replicate Rotorod measurements conformed to a linear fit with $r^2 = 0.91$.

A 6.0-m tower supporting the meteorological equipment was placed 15 m south of the pollen sampling equipment. Meteorological data were sampled continuously at 10 Hz using a datalogger (CR-5000, Campbell Scientific). Wind speed and direction (propeller anemometer 05103, R. M. Young) were measured at 6 m,

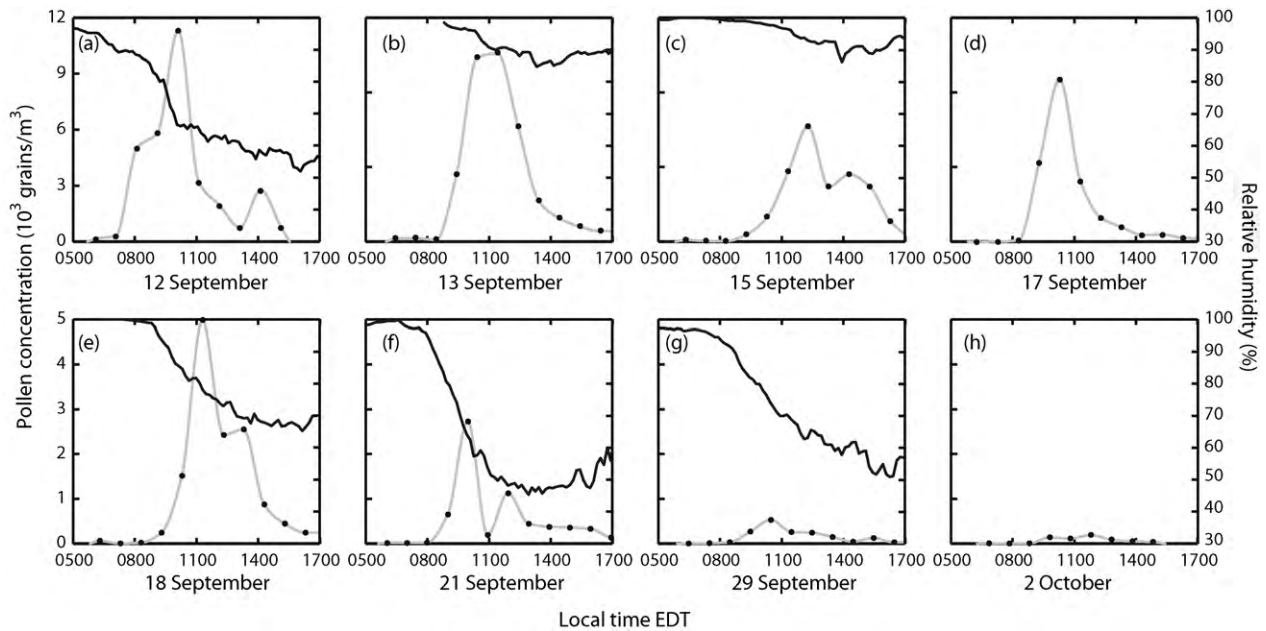


Fig. 1. Time series of *Ambrosia* pollen concentration and relative humidity. Black dots show hourly measurements of pollen concentration from Rotorod samplers placed at $z=2.4$ m. Gray lines are MATLAB-generated interpolation splines displayed for clarity. Black lines show 10-min averages of relative humidity at $z=3$ m. Note change in vertical axis scaling between top and bottom panels. (a) 12 September, 2006; (b) 13 September, 2006; (c) 15 September, 2006; and (d) 17 September, 2006. No meteorological data recorded on this day. (e) 18 September, 2006; (f) 21 September, 2006; (g) 29 September, 2006; and (h) 2 October, 2006. No meteorological data recorded on this day.

temperature and relative humidity (probes HMP45C, Vaisala) at 3 and 5 m, and net radiation (Net Radiometer Q7, Radiation and Energy Systems) at 3 m. Turbulent fluxes were measured using the eddy covariance method with two sonic anemometers (CSAT3, Campbell Scientific) and one Krypton Hygrometer (KH20, Campbell Scientific) at 3 m.

Pollen shed from 10 individual staminate florets was quantified using around 70 h of micro-scale videos that captured the entire period of diurnal pollen release – from closed corolla lobes to the entrainment of the vast majority of pollen grains from the target floret – at 30 fps with a tripod-mounted digital camcorder (DSR-PD170, Sony Electronics) and a reversed telephoto lens. Movement of the inflorescence-bearing *A. artemisiifolia* branch was reduced by wiring it to a metal stake. A length scale for the video was provided by placing a ruler with micrometer-scale markings within the camera's field of view. In these videos, 1–3 staminate florets were visible in the frame. Rather than as a continuous process, erosion of the pollen mass occurs during discrete events, when large aggregates (clumps) of pollen grains break off and are entrained into the atmosphere. Pollen release from individual staminate florets was quantified by fitting circles within voids left by pollen clumps immediately after their erosion from the pollen mass. These voids were visible when comparing video frames captured immediately before and after an erosion event. We assumed that idealized, spherical pollen grains were optimally packed into spherical clumps in order to estimate the number of grains contained in each eroded pollen clump. See Martin et al. (2009) for a detailed description of this analysis technique. A reference length scale was not available for the video capturing pollen release from two florets on 16 September, so the missing length scales were approximated by matching pre-anthesis floret diameters from those videos with reference length scales.

2.2. Model of environmentally mediated asynchronous anther dehiscence

Pollen clump size data describing the entire diurnal period of pollen release (1-s resolution) for 10 staminate florets were aligned

according to the time of initial pollen release. The individual records of diurnal pollen release data were then binned into 30-min intervals and then averaged to create $R(t)$, a mean curve of diurnal pollen release.

In initial runs of our model, total pollen release from 10^6 flowers was simulated based on an assumption that anthesis times of individual flowers show a Gaussian distribution. We used data from Bianchi et al. (1959) to linearly interpolate values for mean and standard deviation of the Gaussian distributions for each input value of relative humidity. We used MATLAB to generate a total pollen release curve that was the summation of the 10^6 normally distributed average pollen release curves, producing time series of total pollen release for values of relative humidity ranging from 20% to 90%. We also used 10-min averages of relative humidity (measured at $z=3$ m above the ground) to generate pollen release curves that considered variation in relative humidity throughout the pollen release period. In this case, each 10-min time increment was assigned a Gaussian distribution of anthesis times generated by the 10-min average value of relative humidity.

3. Results

3.1. Diurnal cycling

A similar diurnal cycle of airborne pollen load has been observed across the species *A. artemisiifolia*, *Ambrosia trifida* (giant ragweed), and *Ambrosia psilostachya* (western ragweed; Jones, 1952; Ogden and Hayes, 1969). Airborne pollen concentration sharply increases in the early morning hours just after sunrise (0700–0900), rises to a peak before 1200, and slowly tapers off throughout the afternoon. Presented here and generally consistent with these observations are eight diurnal series of hourly pollen concentration measurements (Rotorod sampler elevation $z=2.4$ m) obtained on rainless days between 12 September and 2 October (Fig. 1). Maximum recorded airborne pollen concentration occurred at 1100 on 13 September 2006 with a concentration of $\sim 18,000$ grains m^{-3} just above the canopy level ($z=2.0$ m). Peak concentration waned to ~ 600 grains m^{-3} by 2 October 2006, around the time of the first

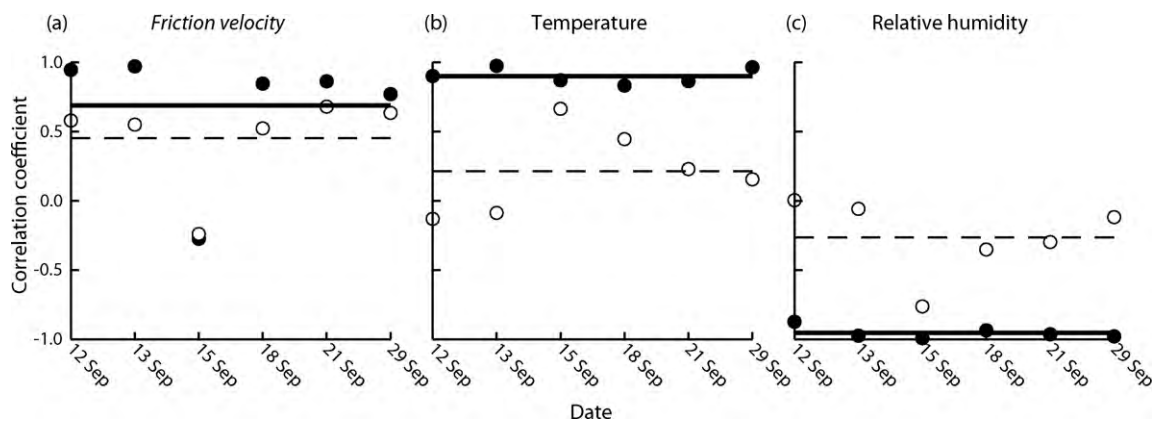


Fig. 2. Correlation coefficients between pollen concentration and meteorological measurements. Data from 6 individual days are plotted. Empty circles are correlations of the meteorological variable with pollen concentrations over the entire diurnal period of measurement. Filled circles are correlations of the pollen concentrations with corresponding meteorological variables only up to that day's maximum in pollen concentration, usually just before mid-day. Horizontal dashed and solid lines indicate mean correlation coefficients for whole-day and before-peak datasets, respectively. (a) Friction velocity (u_*); (b) temperature; and (c) relative humidity.

overnight freeze, although it is unclear to what degree this was a result of changes in overall pollen production, because a majority of the field had been mowed previously for experimental purposes (see Chamecki et al., 2009).

Throughout the measurement period, airborne pollen concentrations showed strong diurnal cycling with mid-morning pollen concentrations typically reaching levels two orders of magnitude above overnight values. Diurnal concentration profiles maintained a strong and consistent negative gradient with the largest concentrations measured at the vegetation canopy ($z = 2.0$ m) and the smallest concentrations measured at $z = 6.0$ m above ground level. Pollen concentrations generally reached a maximum between 1000 and 1100, with the most delayed peak occurring shortly after 1200 on 15 September.

3.2. Bimodality in pollen profiles and relation to meteorological variables

Early research on *Ambrosia* pollen dispersal focused on the large-scale meteorological conditions influencing pollen release. These studies show a close relationship between meteorological variation and *A. psilostachya* pollen release (Bianchi et al., 1959; Ogden and Hayes, 1969). Ogden and Hayes (1969) observed that in select cases, significant pollen loads were observed in the very early morning hours, indicating that the plant is capable of releasing pollen at any time of day, given the proper meteorological conditions. They found no correlation between temperature and hourly pollen production.

Ambrosia pollen concentrations generally decrease after the initial early morning release period. Ogden and Hayes (1969) assumed that airborne pollen observed after this period was re-entrained from leaf surfaces by wind. However, most studies have shown a "fat-tailed" distribution with more pollen load in the second half

of the distribution than would be expected if it were a purely Gaussian process. In some cases, the observed distributions have been bimodal, or at least showing positive skew with a subtle increase in pollen load shortly after mid-day without any correlation to observed meteorological variations either singly or in combination (Jones, 1952; Dingle et al., 1959; Holmes and Bassett, 1963; Ogden and Hayes, 1969; Barnes et al., 2001a,b; Laaidi et al., 2003; Peternel et al., 2006; Stach et al., 2007). To our knowledge, this phenomenon has never received any attention.

Diurnal pollen concentration data collected in our field often showed a bimodal distribution regardless of sampling elevation. This pattern could not be reconciled with any corresponding bimodal distribution of values in the recorded meteorological variables or in the turbulent friction velocity u_* . Relative humidity and temperature are well correlated with the initial rise to the maximum in airborne pollen, but not with variations in pollen load throughout entire diurnal periods (Fig. 2). Correlations with wind magnitude, net radiation, and vapor pressure deficit were similarly poor (data not shown).

Qualitatively, there is a relationship between a slow decrease in relative humidity in the early morning and a delay in the time of the initial peak in pollen: When relative humidity values are low, pollen concentration distributions are bimodal, but a slow or small decrease in relative humidity clearly delays the first airborne pollen concentration peak. Bianchi et al. (1959) show that flowers dehisce over a longer period of time as temperature decreases and relative humidity increases. A distinct bimodal distribution in the pollen concentration time series appears to be inversely related to the rate and degree of drying (decrease in relative humidity) throughout the morning (Fig. 1). This suggests that a slow decrease in relative humidity may be obscuring an underlying, intrinsic bimodal distribution in diurnal pollen concentration by extending

Table 1

Date	Skewness coefficient			
	Rotorod measurements	Model with floral release data $R(t)$	Model with delta function	Model with Gaussian fit to $R(t)$
12 September	0.85	0.65	-0.30	-0.08
13 September	3.04	0.54	-0.08	-0.10
15 September	0.47	0.50	-0.10	-0.14
17 September	2.10	n/a	n/a	n/a
18 September	0.68	0.59	-0.26	-0.23
21 September	0.94	0.74	-0.66	-0.05
29 September	0.93	0.63	-0.23	-0.12
2 October	0.16	n/a	n/a	n/a
Mean	1.15	0.61	-0.27	-0.12

Table 2

Floret	Date recorded	First pollen entrainment time	First pollen entrainment time (min after sunrise)	Final pollen entrainment time	Duration of pollen release (min)	Number of clumps released	Mean clump size (# grains)	Smallest clump size (# grains)	Largest clump size (# grains)	Total number grains released
1	16 September	8:10:29	81.5	12:20:28	250	65	135	3	1330	8796
2	16 September	8:06:12	77.2	1:00:45	295	118	61	1	1915	7212
3	17 September	8:24:35	94.6	13:42:32	318	62	168	1	2262	10411
4	17 September	8:19:10	89.2	13:08:45	290	54	80	1	543	4319
5	17 September	8:22:00	92.0	14:40:22	378	83	109	1	1463	9012
6	18 September	8:22:58	92.0	12:44:27	261	86	47	1	500	4048
7	18 September	8:19:41	88.7	12:44:27	265	66	76	1	579	5047
8	18 September	9:45:39	174.7	13:53:15	248	17	162	1	1372	2753
9	18 September	9:43:08	172.1	12:54:20	191	10	249	4	1687	2486
10	21 September	8:52:00	118.0	14:34:00	342	50	34	1	264	1722
Mean		8:38:35	108.0	13:22:20	284	61	112	1	1191	5581
Standard deviation			36		53	32	67	1	681	3070

the range of individual pollen release times in our field. Even when a secondary peak is not clear, all the pollen concentration time series have large, positive values of Fisher's skewness coefficient (moment skewness), indicating that the pollen distributions are "fat-tailed" after the time of mean pollen release, generally around mid-day (Table 1).

The diurnal time series of pollen concentration can be generally divided into monomodal and bimodal distributions. On 13 September, relative humidity fell to around 90% before 1000, and the pollen concentration was clearly monomodal. On 12 and 21 September, relative humidity fell to around 50%. On 29 September, relative humidity fell to around 80% by 1000, and the distribution was relatively monomodal except for a slight increase after 1500, about 5 h after the first peak. Although relative humidity decreased slowly on this day, it did eventually drop quite low (from 100% in early morning to 50% by mid-afternoon). The second peak may have appeared because the humidity levels eventually fell enough to initiate another burst of pollen release. The data from 15 September appears to be an exception to this trend. Relative humidity fell to only around 90% before 1000, and pollen concentrations appear bimodal. However, there were anomalous decreases in measurements of u_z and wind magnitude during the lag period between the primary and secondary peaks, so it is possible that the underlying pollen concentration is more closely monomodal, with pollen concentrations decreasing with atmospheric turbulence. Pollen concentration on 18 September appears to be a transitional case, and relative humidity fell to only around 85% before 1000. Late-morning hours with 80–85% relative humidity may be the threshold at which bimodal features appear.

3.3. Pollen release at the floral scale

The diurnal pollen release process seen in the videos has been described in general in Martin et al. (2009). The corolla lobes remain tightly closed until just before anther dehiscence. The swollen anthers then extend out of the floret, gradually opening the corolla lobes. At anther dehiscence, a substantial wad of pollen is presented to the wind. Usually, there is a large, initial release of pollen at anthesis as the anthers burst open, but depending on the wind, pollen can remain on the floret for some time. The average delay between sunrise and the first pollen entrainment was 108 min (Table 2). A secondary period of increased pollen entrainment follows after some delay as the extending pistillodium extrudes a wad of pollen. The mean duration of the entire dehiscence process of a single flower is 4.7 h. The pollen release process is dominated by the erosion and atmospheric entrainment of large pollen clumps from the pollen mass, which is extruded from the floret's interior. Pollen clumps removed from the florets contained an average of 67 grains. Although single-grain entrainments did occur, they were exceedingly rare, consistent with previous observations of pollen release in this species (Fig. 3).

A bimodal distribution is visible in pollen entrainments from individual florets (Fig. 3a). The initial peak comes shortly after anthesis as a direct result of the early morning dehiscence of the anthers. As the anthers continue to rupture, a mass of pollen grows and is simultaneously eroded by the turbulent wind. This process continues until the protruding mass is completely eroded. A period of calm follows with little to no extrusion of pollen from within the floret, and hence very little entrainment. After the lag period, pollen remaining in the floret is slowly extruded by the growing pistillodium, which becomes visible as it extends along the central axis of the flower. At maximum extension, the pistillodium protrudes from the flower, where the pollen on its surface can be swept away by the wind. It is important to note that less than 50% of total pollen release occurs during the 30 min following anthesis (Fig. 3a). The

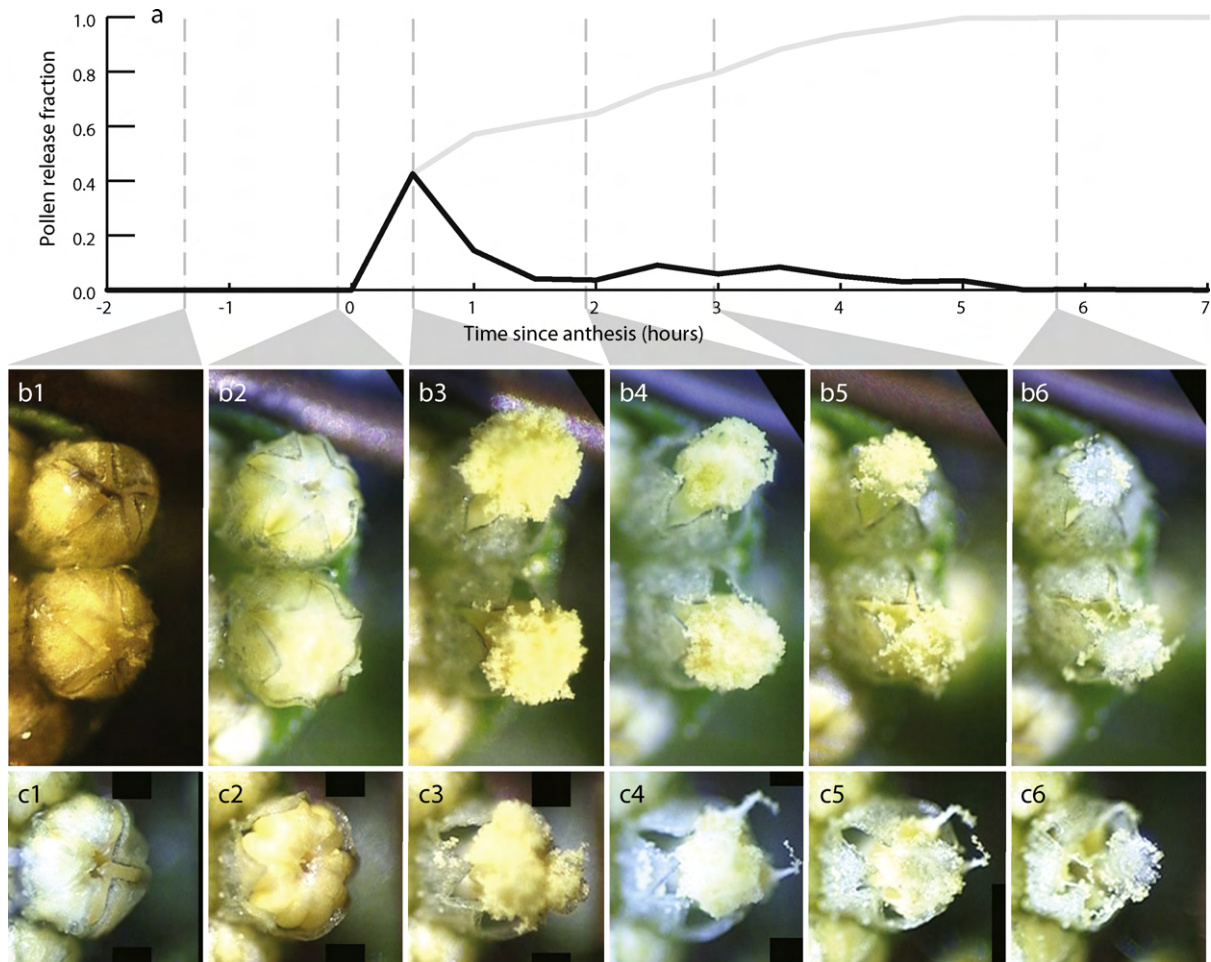


Fig. 3. Pollen release from individual florets. (a) The normalized and averaged data from all 10 florets analyzed. Black line is the average pollen release curve $R(t)$. Solid gray line is the running total of normalized pollen release. Dashed gray lines correspond to the approximate temporal location in $R(t)$ of the frames from (b1–6) and (c1–6). (b1) Two florets imaged in a single video on 17 September. Hours before anthesis, dehiscent florets begin to swell and yellow as the anthers press against the corolla lobes. (b2) Just before anthesis, distended anthers part the corolla lobes and protrude from the floret. (b3) The duration of anthesis is typically less than 2 min. During this time, the anther locules burst, and a wad of fresh pollen is pushed forward out of the floral cavity. (b4) Wind erosion of the pollen wad begins immediately after anthesis and continues throughout the day. The pollen is removed in large clumps typically consisting of over 100 individual grains (Table 2). (b5) Approximately 3 h after anthesis, the extending pistillodium becomes visible, extruding pollen from the interior of the floret. (b6) The pistillodium completes its extension, and wind removes the remaining pollen from its trichomes. (c1–6) The same process depicted in a single floret imaged on 18 September.

majority of pollen is released during the slow erosion of the pollen mass, which lasts about 5 h.

3.4. Model results under theoretical conditions of constant relative humidity

We developed a simple model to test our hypothesis that changes in the degree of bimodality in the diurnal pollen concentration time series could be explained by varying statistical distributions of anthesis times of individual staminate florets across the field. Bianchi et al. (1959) report time series data of the fraction of total florets dehisced versus the time of exposure to steady conditions of 20, 40, 60, 70, and 80% relative humidity. Error functions (integrals of Gaussian/normal distributions) fit their data of humidity versus fraction of total dehiscence extremely well (r^2 ranged from 0.985 to 0.999). This indicates that when relative humidity is constant, anther dehiscence in individual staminate florets is a random phenomenon normally distributed around some mean and characteristic variance. We fitted error functions to their data to find the standard deviation and mean of the normal distributions they reported for 20, 40, 60, and 70% relative humidity (Fig. 4). Linear interpolation between these points gave a mean μ_k and

standard deviation σ_k for all possible values of relative humidity:

$$\mu_k = 2.255RH_k, \quad \sigma_k = 0.539RH_k, \quad (1)$$

where RH_k is the measured value of relative humidity averaged over time interval k . Both fits assumed a linear relationship between the variables and a y -intercept of 0. Physically, the assumption is that pollen release begins and ends instantaneously when the relative humidity is equal to zero. The best linear fits gave y -intercepts of less than zero, which were not physical. However, using those relationships in place of the fits with $y(0) = 0$ did not have any significant effect on the model outcome.

This model of environmentally mediated asynchronous anther dehiscence uses an average of the 10 pollen release time series from our video analysis. We aligned the initial dehiscence times for each floret, averaged the pollen release measurements in 15-min bins, and then took an average of the 10 aligned release curves. This function, $R(t)$, is a mean of the 10 floral datasets and is plotted in Fig. 3a, which shows that the average pollen release curve is decidedly skewed with a primary peak followed by an extended period of release. This is observed in the videos of pollen release from staminate florets. A time interval of about 5 h was required for the entire process. The model assumes that each floret in the field releases pollen according to $R(t)$ and that pollen release depends

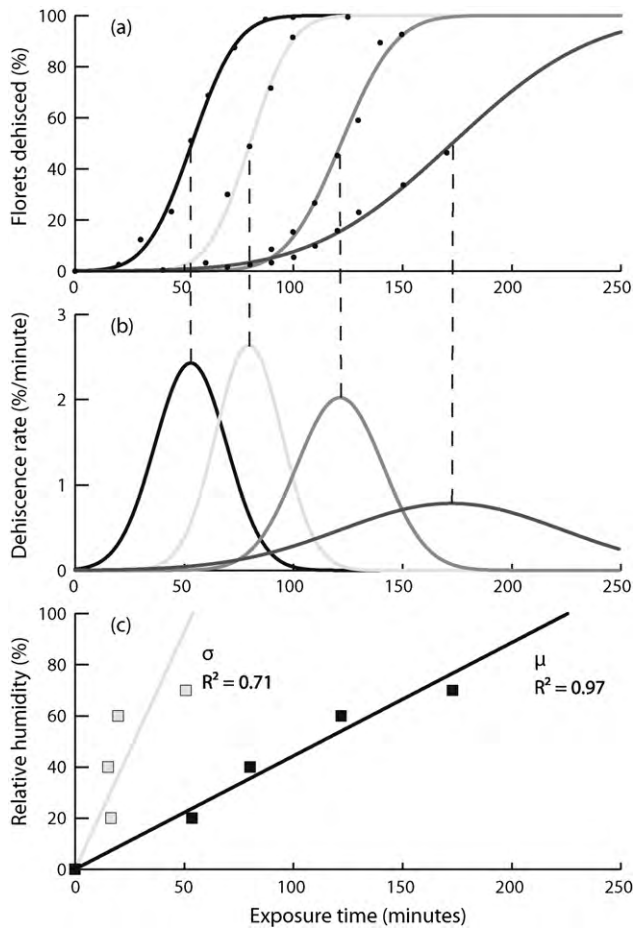


Fig. 4. Linear interpolation of data from Bianchi et al. (1959). (a) Black dots depict the original data on floret dehiscence versus time for constant values of relative humidity. Curves are error functions fitted to the data. From left to right: 20, 40, 60, and 70% relative humidity. (b) Time derivatives of the error functions from (a) with mean dehiscence times illustrated. (c) Linear interpolation of the relationships between relative humidity and the values of μ and σ determined from the best fits to the Bianchi et al. (1959) data.

only on relative humidity and time of sunrise (time $t=0$ in the model).

For a range of constant values of relative humidity, we randomly generated dehiscence times for 10^6 florets from the Gaussian function:

$$D_k(t) = \frac{1}{\sigma_k \sqrt{2\pi}} e^{-1/2(t-\mu_k/\sigma_k)^2}. \quad (2)$$

The mean time μ_k (delay after some arbitrary time $t=0$) and standard deviation σ_k are constant and interpolated from Bianchi et al. (1959) according to Eq. (1). We generated a data structure that is the summation (normalized by its maximum value) of the 10^6 average pollen release curves with each curve initializing at the corresponding dehiscence time. This simulates a field of plants with 10^6 florets opening randomly, according to a Gaussian distribution, in conditions of constant relative humidity ($\Delta t \sim 8$ h). Varying relative humidity between 20 and 90% in this simulation delayed the initial peak in pollen release by around 3 h (Fig. 5). Our results further show that in dry conditions, the average pollen release curve taken from the floral videos is still recognizable, and the secondary peak in pollen release activity is easily visible. In more humid conditions, the initial and secondary peaks of pollen release begin to coalesce. At 90% relative humidity, the input data are almost unrecognizable, and the total pollen release curve looks like a skewed Gaussian distribution. We argue that humidity changes in the early morning determine the synchronization of anthesis across the field, which has a direct influence on the overall appearance of the pollen distribution above the canopy. We hypothesize that this effect is always present in the airborne pollen concentration time series – either in a clear bimodal distribution or, when field-wide anther dehiscence shows relatively little synchronization, in the form of a highly skewed normal distribution.

3.5. Model results under real-world conditions of varying relative humidity

Next we investigated whether our hypothesis of environmentally mediated asynchronous dehiscence could explain direct observations of airborne *Ambrosia* pollen concentration. We extended the model to use 10-min averages of measured relative humidity, as well as the floral release data and a few simple

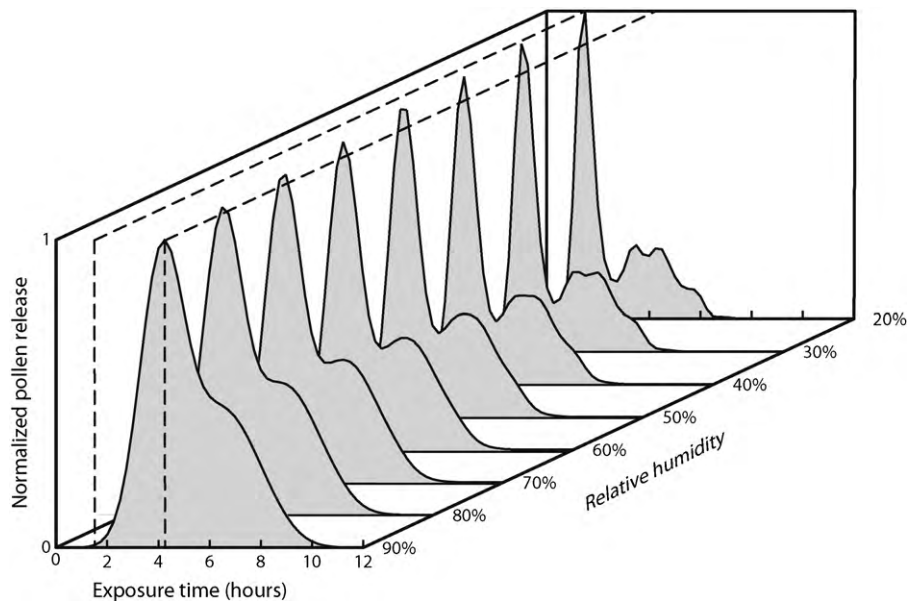


Fig. 5. Results from the model simulation pollen release from 10^6 florets under conditions of constant relative humidity. Dashed lines illustrate the large difference in peak pollen release time for 20 and 90% relative humidity.

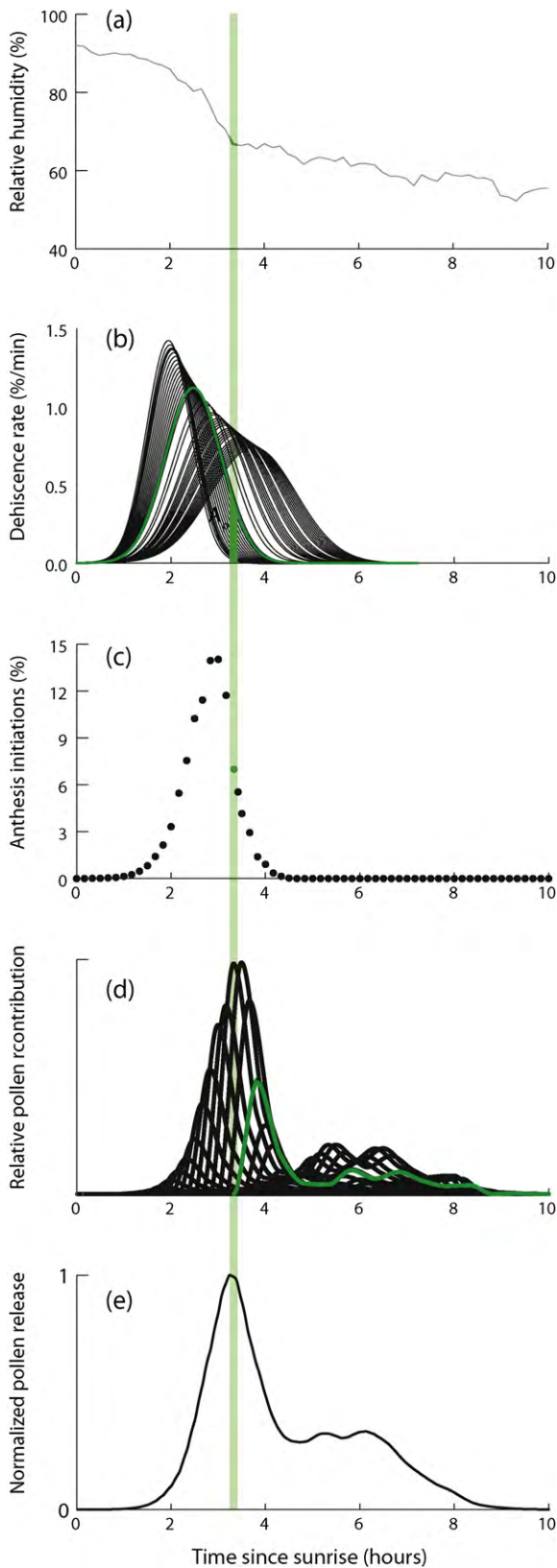


Fig. 6. Descriptive illustration of pollen release model. The vertical green bar highlights time interval k . (a) Mean value of relative humidity over each 10-min interval k determines the mean μ_k and variance σ_k of the Gaussian function of anthesis probability. (b) Plots of all Gaussian distributions of anthesis probability used in this run of the model. The green curve is the Gaussian distribution described by μ_k and σ_k . The green region beneath the curve is A_k . (c) The normalized schedule of anthesis initiations with A_k represented as a solid green circle. (d) Black lines are all average pollen release curves $R(t)$ used in the model. One curve

assumptions, to predict relative pollen concentration above the field (Fig. 6).

The model estimates the fraction of all dehiscent florets initiating anthesis during each time interval, and then calculates the sum of the pollen release contributions from all the individual florets that are releasing pollen during that interval. Our major assumption is that the field has no memory of previous values of relative humidity: For each time step in the model, the fraction of flowers initiating anthesis during that interval is determined solely by the mean relative humidity during that time interval. The relative fraction of flowers initiating anthesis during the time interval k is the integral of the Gaussian curve of dehiscence rate, during that interval k , determined from the interval's mean relative humidity RH_k . More formally,

$$A_k = \int_k^{k+\Delta t} D_k(t) dt, \quad (3)$$

where t is the time elapsed since sunrise, A_k is the relative fraction of flowers initiating anther dehiscence during time interval k , Δt is the duration of time interval k , and $D_k(t)$ is the Gaussian distribution of dehiscence rate, which depends directly on values of μ_k and σ_k^2 determined for interval k from Eq. (1). Because $\sum_{k=1}^Z A_k$ (where Z is the total number of time intervals in the model run) does not yield 1, A_k is only the relative fraction of florets initiating anthesis during interval k . For the true fraction of anthesis initiations predicted by the model, A_k must be normalized by this sum. Because this operation has no effect on the model results due to normalization of the final model output, this normalization is not performed in the model.

Output from the model is $P(t)$, the fraction of all pollen grains released in the field as a function of time:

$$P(t) = \sum_{k=1}^Z [A_k \cdot R(t - k\Delta t)], \quad (4)$$

where $R(t)$ is the mean floral release curve from the analysis of the digital videos shown in Fig. 3a.

The model used 10-min averages ($\Delta t = 10$ min) of relative humidity to predict normalized, hourly Rotorod measurements of pollen concentration. Six runs of the model (corresponding to the 6 days for which we had both meteorological data and Rotorod data) yielded 69 hourly averages of predicted pollen concentration just above canopy height ($z = 2.4$ m). The model fit the experimental data with $r^2 = 0.71$ ($n = 69$).

We also tested the dependence of the model on the floral release curve generated during the analysis of the digital videos with two types of control runs. In the first, the model ran as described, but for $R(t)$ we substituted a delta function as the average floral release curve calculated from the digital videos (Fig. 7). This tested the assumption that airborne pollen concentration depends directly on the relative number of anther dehiscence events occurring concurrently by removing the data about how pollen release from the florets varies with time. These runs of the model yielded an extremely poor fit to the hourly airborne pollen concentrations ($r^2 = 0.09$). To test the dependence of the model on the secondary peak in the average floral pollen release curve, which is presumably a product of the extension of the pistillodium, we attempted to remove this effect by calculating the best Gaussian fit to $R(t)$ ($r^2 = 0.84$) and substituting this function for $R(t)$ in the model.

initiates in each time interval. Each curve is scaled by a fraction of anthesis initiations occurring during that interval. The green curve is the contribution from interval k . (e) Final model output $P(t)$ is the normalized sum of pollen release contributions to each time interval from (d). (For interpretation of the references to color in this figure legend, the reader is referred to the web version of this article.)

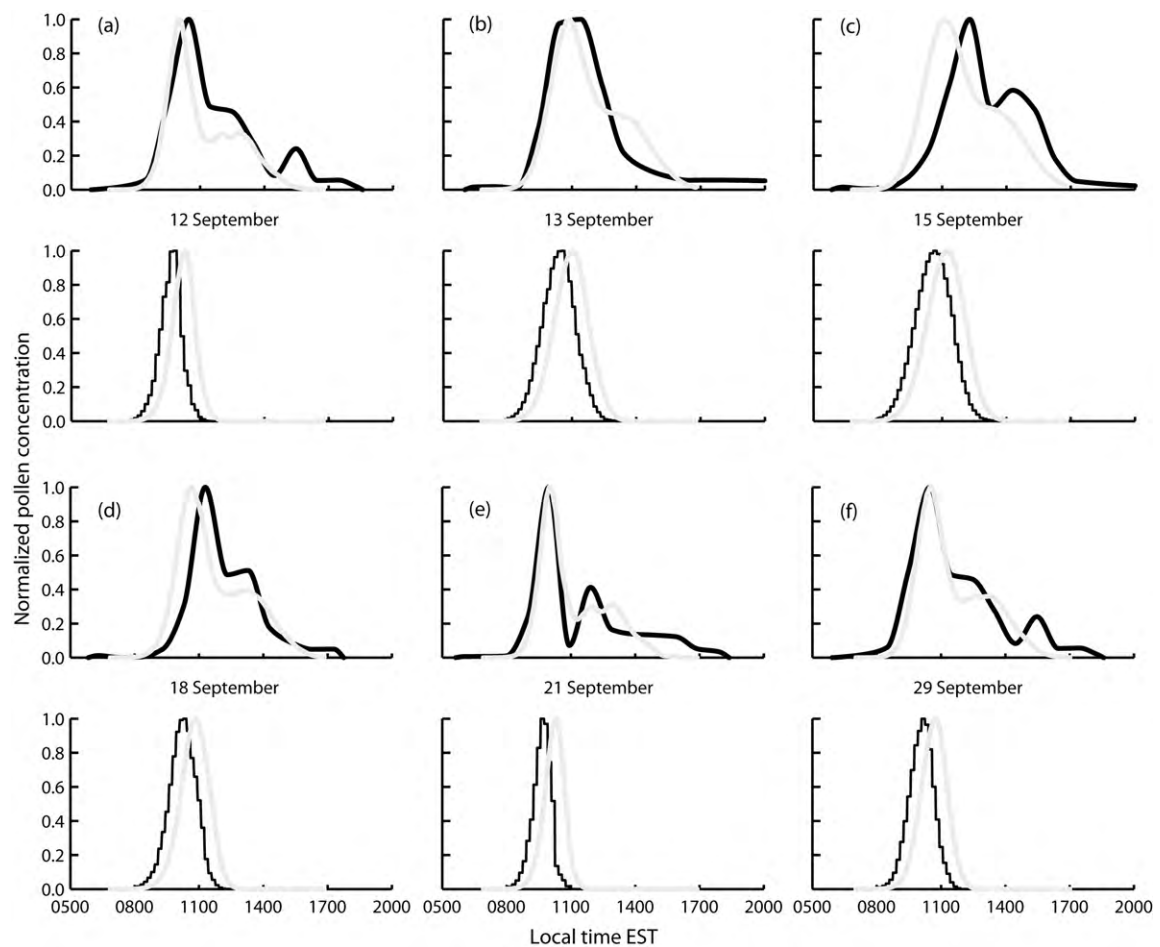


Fig. 7. Results of the pollen release model with varying humidity. Black curve in each upper pane is the splined interpolation through the original Rotorod pollen concentration data. Gray curve in each upper pane is the output of the complete pollen release model utilizing the average pollen release curve $R(t)$. Thin black curve in each lower pane is the model output when substituting a delta function for $R(t)$. Gray curve in each lower pane is the model output when substituting a Gaussian function fitted to $R(t)$. (a) 12 September, 2006; (b) 13 September, 2006; (c) 15 September, 2006; (d) 18 September, 2006; (e) 21 September, 2006; and (f) 29 September, 2006.

Control runs with this Gaussian fit to floral release curve $R(t)$ yielded somewhat better results than runs with the delta function. Still, the fit of $r^2 = 0.29$ represents significantly worse agreement with measured pollen concentrations than when utilizing $R(t)$, the true floral pollen release data from the digital videos.

4. Discussion

We constructed a model to investigate whether data from Bianchi et al. (1959) detailing the relationship between species-specific anther dehiscence and relative humidity alone could predict concentration of pollen above a dense field of *A. artemisiifolia*. Results from the model show that both the temporal changes in relative humidity and the pollen release data from the flower are needed to achieve optimum agreement with the pollen concentration measurements. This study also shows that pollen release from individual staminate florets is always bimodal. This intrinsic bimodality can be obscured when anther dehiscence is desynchronized across an entire field of florets. The degree of synchronization is determined by variations in relative humidity. In addition, we show that the diurnal pattern of airborne pollen concentration above the *A. artemisiifolia* canopy is very closely related to the extension of the staminate floret's pistillodium, the rapid physiological development of which may be a response to environmental stimuli. It is interesting that such a small organ (diameter $\sim 100 \mu\text{m}$) has such a profound effect at the field scale (area $\sim 6 \times 10^4 \text{ m}^2$).

There is a delay of about 1 h between the average peak in pollen release recorded on video and the average peak in airborne pollen concentration from the Rotorod samplers. This delay is curious and may indicate some sampling bias in flower choice for the pollen release analysis. Bianchi et al. (1959) noted that dehiscent florets become distinguishable from others a few hours before anthesis by developing a yellow color. We chose target florets for digital videography before sunrise and so would have preferentially chosen florets that were the most obvious candidates to release pollen. If this scenario were the case, the bias would likely be removed by aligning pollen release datasets to time since anthesis, as evidenced by the excellent agreement of the model with the timing of the primary peaks in diurnal airborne pollen concentration. A less likely possibility is that the aforementioned delay is a result of large pollen clumps settling onto surrounding vegetation and then being re-entrained into the atmosphere after some time. Bianchi et al. (1959) reported that process as being characteristic of the pollen release process, but no data are available concerning the resting period. We did observe a homogenous layer of *A. artemisiifolia* pollen coating the surface of vegetation in the field at mid-day. These grains were presumably held in place by static forces or through the interaction of leaf trichomes with the rough exine of the pollen grains. It is possible that the resting period of pollen clumps on vegetative surfaces plays some role in the diurnal pollen release process. However, we have shown that a large majority of the temporal variation in airborne pollen concentration can be explained by our model without any consideration of a pollen resting period.

It is surprising that such good predictions result from our simple and intuitive model, especially considering that there are no calibrated parameters and that wind velocity and the shape of the field are not accounted for. However, a number of factors likely contribute to model error. The model actually predicts the timing of pollen release, not airborne pollen concentration above the canopy, which must depend on events between anther dehiscence and final pollen transport above the canopy. A number of factors strongly influence these events, including wind speed and turbulent conditions. Actual airborne concentration will be influenced by the total production of pollen, stability of the boundary layer and turbulent conditions, and variability in pollen entrainment and settling (Tyldesley, 1973; Finnigan, 2000; Aylor, 2005). Pollen clumping also has a complex influence on atmospheric transport (Martin et al., 2009). In addition, we assumed linear relations between relative humidity and mean dehiscence time from data in Bianchi et al. (1959), although clearly this assumption is not appropriate at higher values of relative humidity. This may significantly affect model predictions during the early morning hours. Bianchi et al. (1959) also showed that overnight exposure to different temperatures will affect the distribution of anthesis times once the dehiscence process begins, but this factor was not considered here. Finally, the pollen release dataset is stochastic, as it is based on observations of only 10 florets and then extrapolated to model field scale pollen concentration, the combined influence of an estimated 10^9 florets. Further observation of flower scale pollen entrainment should yield a more robust average pollen release curve. Surprisingly, though, the model results were not greatly affected by utilizing different combinations of normalization and alignment of the individual floral datasets to calculate $R(t)$.

Previous attempts to correlate meteorological conditions with pollen concentrations may have failed due to a lack of consideration of the relationship between the meteorological conditions and species-specific anemophilous floral structure and behavior. For example, the ubiquitous bimodal distribution observed in concentration profiles of maize pollen (Jarosz et al., 2003, 2005; van Hout et al., 2008) may result from a physiological action in the corn anther. Our study suggests that floral biology (in this case, the role of the pistillodium) cannot be ignored. A simple model that accounts only for the relationship between relative humidity and anthesis timing and the effect of the pistillodium on timing of pollen release events predicts hourly airborne pollen concentrations better than correlations with many other meteorological variables.

Species-specific models of pollen release allow complete models of wind dispersion of pollen from anemophilous plants. A thorough understanding of the diurnal cycles of pollen release and dispersion from *A. artemisiifolia* will help to predict both the movement of its genes between populations and the local and long-distance dispersal of its pollen, which could mitigate its impact on sensitive allergy sufferers by improving allergy forecasts. The ability of a plant species to disperse its pollen can have a direct impact on the generic health of its populations (Nakanishi et al., 2009). A better understanding of differences between the mechanisms of pollen release and dispersal across the genus *Ambrosia* may provide clues about how *A. artemisiifolia* and *A. trifida* have proliferated while the invasive performance of other *Ambrosia* species has remained unremarkable.

Acknowledgements

This project was supported by U.S.–Israel Binational Science Foundation grant 2006214 and National Science Foundation award BES-0119903. Many thanks to P. Goldstein, D. Martinez, J. Chen, and C. Chen for their invaluable microscope work. Thanks to B. DeTemple for his expertise in the optical setup. Thanks to C. Higgins,

M. Spicknall, E. Toney, P. Delano, and S. Featherstone for their assistance in the field experiment. We are indebted to S. Isard for his critical reading of the manuscript.

References

- Alba, F., Diaz de la Guardia, C., Comtois, P., 2000. The effect of meteorological parameters on diurnal patterns of airborne olive pollen concentration. *Grana* 39, 200–208.
- Arritt, R.W., Clark, C.A., Goggi, A.S., Sanchez, H.L., Westgate, M.E., Riese, J.M., 2007. Lagrangian numerical simulations of canopy air flow effects on maize pollen dispersal. *Field Crops Research* 102, 151–162.
- Aylor, D.E., Schultes, N.P., Shields, E.J., 2003. An aerobiological framework for assessing cross-pollination in maize. *Agricultural and Forest Meteorology* 119, 111–129.
- Aylor, D.E., 2005. Quantifying maize pollen movement in a maize canopy. *Agricultural and Forest Meteorology* 131, 247–256.
- Barnes, C., Pacheco, F., Landuyt, J., Hu, F., Portnoy, J., 2001a. The effect of temperature, relative humidity and rainfall on airborne ragweed pollen concentrations. *Aerobiologia* 17, 61–68.
- Barnes, C., Pacheco, F., Landuyt, J., Hu, F., Portnoy, J., 2001b. Hourly variation of airborne ragweed pollen in Kansas City. *Annals of Allergy, Asthma, and Immunology* 86, 166–171.
- Bass, D.J., Delpech, V., Beard, J., Bass, P., Walls, R.S., 2000. Late summer and fall (March–May) pollen allergy and respiratory disease in Northern New South Wales, Australia. *Annals of Allergy, Asthma, and Immunology* 85, 374–381.
- Bassani, M., Pacini, E., Franchi, G.G., 1994. Humidity stress responses in pollen of anemophilous and entomophilous species. *Grana* 33, 146–150.
- Beckie, H.J., Hall, L.M., 2008. Simple to complex: modelling crop pollen-mediated gene flow. *Plant Science* 175, 615–628.
- Bianchi, D.E., Schwemmin, D.J., Wagner, W.H., 1959. Pollen release in the common ragweed (*Ambrosia artemisiifolia*). *Botanical Gazette* 120, 235–243.
- Cecchi, L., Torrigiani Malaspina, T., Albertini, R., Zanca, M., Ridolo, E., Usberti, I., Morabito, M., Dall'Aglio, P., Orlandini, S., 2007. The contribution of long-distance transport to the presence of *Ambrosia* pollen in central northern Italy. *Aerobiologia* 23, 145–151.
- Chamecki, M., Meneveau, C., Parlange, M.B., 2009. Large eddy simulation of pollen transport in the atmospheric boundary layer. *Journal of Aerosol Science* 40, 241–255.
- Chauvel, B., Dessaint, F., Cardinal-Legrand, C., Bretagnolle, F., 2006. The historical spread of *Ambrosia artemisiifolia* L. in France from herbarium records. *Journal of Biogeography* 33, 665–673.
- Comtois, P., Gagnon, L., 1988. Pollen concentration and frequency of pollinosis symptoms: a method of determination of the clinical threshold. *Revue Française de Allergologie et de Immunologie Clinique* 28, 279–286.
- Crimi, P., Macrina, G., Folli, C., Bertoluzzo, L., Bricchetto, L., Caviglia, I., Fiorina, A., 2004. Correlation between meteorological conditions and *Parietaria* pollen concentration in Alassio, north-west Italy. *International Journal of Biometeorology* 49, 13–17.
- Dahl, A., Strandhede, S.O., Wihl, J.-A., 1999. Ragweed—an allergy risk in Sweden? *Aerobiologia* 15, 293–297.
- Dingle, A.N., Gill, G.C., Wagner Jr., W.H., Hewson, E.W., 1959. The emission, dispersion, and deposition of ragweed pollen. *Advances in Geophysics* 6, 367–386.
- Dow, B.D., Ashley, M.V., 1998. Factors influencing male mating success in bur oak, *Quercus macrocarpa*. *New Forests* 15, 161–180.
- Ellstrand, N.C., Schierenbeck, K.A., 2000. Hybridization as a stimulus for the evolution of invasiveness in plants? In: *Proceedings of the National Academy of Sciences*, USA 97 7043–7050.
- Finnigan, J., 2000. Turbulence in plant canopies. *Annual Reviews of Fluid Mechanics* 32, 519–571.
- Friedman, J., Barrett, S.C.H., 2008. High outcrossing in the annual colonizing species *Ambrosia artemisiifolia* (Asteraceae). *Annals of Botany* 101, 1303–1309.
- Fumanal, B., Chauvel, B., Bretagnolle, F., 2007. Estimation of pollen and seed production of common ragweed in France. *Annals of Agricultural and Environmental Medicine* 14, 233–236.
- Galán, C., Alcázar, P., Cariñanos, P., García, H., Domínguez-Vilches, E., 2000. Meteorological factors affecting daily urticaceae pollen counts in southwest Spain. *International Journal of Biometeorology* 43, 191–195.
- Genton, B.J., Shykoff, A., Giraud, T., 2005. High genetic diversity in French invasive populations of common ragweed, *Ambrosia artemisiifolia*, as a result of multiple sources of introduction. *Molecular Ecology* 14, 4275–4285.
- Gergen, P.J., Turkeltaub, P.C., Kovar, M.G., 1987. The prevalence of allergic skin test reactivity to eight common aeroallergens in the U.S. population: results from the second National Health and Nutrition Examination Survey. *Journal of Allergy and Clinical Immunology* 80, 669–679.
- Holmes, R.M., Bassett, I.J., 1963. Effect of meteorological events on ragweed pollen count. *International Journal of Biometeorology* 7, 27–34.
- Jarosz, N., Loubet, B., Durand, B., Foueillassar, X., Huber, L., 2005. Variations in maize pollen emission and deposition in relation to microclimate. *Environmental Science and Technology* 39, 4377–4384.
- Jarosz, N., Loubet, B., Durand, B., McCartney, A., Foueillassar, X., Huber, L., 2003. Field measurements of airborne concentration and deposition rate of maize pollen. *Agricultural and Forest Meteorology* 119, 37–51.

- Jones, A.M., Harrison, R.M., 2004. The effects of meteorological factors on atmospheric bioaerosol concentrations—a review. *Science of the Total Environment* 326, 151–180.
- Jones, M.D., 1952. Time of day of pollen shedding of some hay fever plants. *Journal of Allergy* 23, 247–258.
- Keijzer, C.J., 1983. Hydration changes during anther development. In: Mulcahy, D.L., Ottaviano, E. (Eds.), *Pollen, Biology and Implications for Plant Breeding*. Elsevier Biomedical, New York, pp. 197–201.
- Keijzer, C.J., 1999. Mechanisms of Angiosperm anther dehiscence, a historical review. In: Clement, C., Pacini, E., Audran, J.-C. (Eds.), *Anther and Pollen: From Biology to Biotechnology*. Springer-Verlag, Berlin, pp. 56–67.
- Kiss, L., Beres, I., 2006. Anthropogenic factors behind the recent population expansion of common ragweed (*Ambrosia artemisiifolia* L.) in Eastern Europe: is there a correlation with political transitions? *Journal of Biogeography* 33, 2154–2157.
- Laaidi, M., Laaidi, K., Besancenot, J.-P., Thibaudon, M., 2003. Ragweed in France: an invasive plant and its allergenic pollen. *Annals of Allergy, Asthma, and Immunology* 91, 195–201.
- Laursen, S.C., Reiners, W.A., Kelly, R.D., Gerow, K.G., 2007. Pollen dispersal by *Artemisia tridentata* (Asteraceae). *International Journal of Biometeorology* 51, 465–481.
- Luna, V.S., Figueroa, J.M., Baltazar, B.M., Gomez, R.L., Townsend, R., Schoper, J.B., 2001. Maize pollen longevity and distance isolation requirements for effective pollen control. *Crop Science* 41, 1551–1557.
- Makra, L., Juhasz, M., Borsos, E., Beczi, R., 2004. Meteorological variables connected with airborne ragweed pollen in Southern Hungary. *International Journal of Biometeorology* 49, 37–47.
- Martin, M.D., Chamecki, M., Brush, G.S., Meneveau, C., Parlange, M.B., 2009. Pollen clumping and wind dispersal in an invasive angiosperm. *American Journal of Botany* 96, 1703–1711.
- McCartney, H.A., Lacey, M.E., 1991. Wind dispersal of pollen from crops of oilseed rape (*Brassica napus* L.). *Journal of Aerosol Science* 22, 467–477.
- Munoz, A.F., Silva, I., Tormo, R., Moreno, A., Tavira, J., 2000. Dispersal of Amaranthaceae and Chenopodiaceae pollen in the atmosphere of Extremadura (SW Spain). *Grana* 39, 56–62.
- Nakanishi, A., Tomaru, N., Yoshimaru, H., Manabe, T., Yamamoto, S., 2009. Effects of seed- and pollen-mediated gene dispersal on genetic structure among *Quercus salicina* saplings. *Heredity* 102, 182–189.
- Norris-Hill, J., 1999. The diurnal variation of Poaceae pollen concentrations in a rural area. *Grana* 38, 301–305.
- Ogden, E.C., Hayes, J.V., 1969. Diurnal patterns of pollen emission in *Ambrosia*, *Phleum*, *Zea*, and *Ricinus*. *American Journal of Botany* 56, 16–21.
- Ostroumov, A.I., 1971. Hypersensitivity caused by Ambrosia pollen in the Kuban area (Krasnodar Region). *Allergie und Immunologie (Leipzig)* 17, 202–207.
- Payne, W.W., 1963. The morphology of the inflorescence of ragweeds (*Ambrosia-Franseria*: Compositae). *American Journal of Botany* 50, 872–880.
- Percival, M., 1950. Pollen presentation and pollen collection. *New Phytologist*, 4940–4963.
- Peternel, R., Culig, J., Hrga, I., Hercog, P., 2006. Airborne ragweed (*Ambrosia artemisiifolia* L.) pollen concentrations in Croatia, 2002–2004. *Aerobiologia* 22, 161–168.
- Roitt, I., Brostoff, J., Male, D., 1996. *Immunology*. Mosby-Year Book Europe, London, England.
- Rybnczek, O., Jäger, S., 2001. *Ambrosia* (ragweed) in Europe. *Allergy and Clinical Immunology International: Journal of the World Allergy Organisation* 13, 60–66.
- Saar, M., Gudžinskas, Z., Ploompuu, T., Linno, E., Minkien, Z., Motiekaitytė, V., 2000. Ragweed plants and airborne pollen in the Baltic States. *Aerobiologia* 16, 101–106.
- Šikoparija, B., Radišić, P., Pejak, T., Šimić, S., 2006. Airborne grass and ragweed pollen in the southern Pannonian Valley—consideration of rural and urban environment. *Annals of Agricultural and Environmental Medicine* 13, 263–266.
- Šikoparija, B., Smith, M., Skjøth, C.A., Radišić, P., Milkovska, S., Šimić, S., Brandt, J., 2009. The Pannonian plain as a source of *Ambrosia* pollen in the Balkans. *International Journal of Biometeorology* 53, 263–272.
- Singer, B.D., Ziska, L.H., Frenz, D.A., Gebhard, D.E., Straka, J.G., 2005. Increasing Amb a 1 content in common ragweed (*Ambrosia artemisiifolia*) pollen as a function of rising atmospheric CO₂ concentration. *Functional Plant Biology* 32, 667–670.
- Solomon, W.R., 1984. Aerobiology of pollinosis. *Journal of Allergy and Clinical Immunology* 74, 449–461.
- Stach, A., Smith, M., Skjøth, C.A., Brandt, J., 2007. Examining *Ambrosia* pollen episodes at Poznan (Poland) using back-trajectory analysis. *International Journal of Biometeorology* 51, 275–286.
- Stinson, K.A., Bazzaz, F.A., 2006. CO₂ enrichment reduces reproductive dominance in competing stands of *Ambrosia artemisiifolia* (common ragweed). *Oecologia* 147, 155–163.
- Stirton, C.H., 1983. Nocturnal petal movements in the Asteraceae. *Bothalia* 14, 1003–1006.
- Sugaya, A., Tsuda, T., Ohguchi, H., 1997. Marked increase of atmospheric pollen dispersion of ragweed (*Ambrosia* spp.): annual changes in atmospheric pollen counts of major allergen plants in autumn in Saitama Prefecture. *Arerugi* 46, 585–593.
- Tanaka, O., Wada, H., Yokoyama, T., Murakami, H., 1987. Environmental factors controlling capitulum opening and closing of dandelion, *Taraxacum albidum*. *Plant Cell Physiology* 28, 727–730.
- Taramarcaz, P., Lambelet, C., Clot, B., Keimerd, C., Hauser, C., 2005. Ragweed (*Ambrosia*) progression and its health risks: will Switzerland resist this invasion? *Swiss Medical Weekly* 138, 538–548.
- Tyldesley, J.B., 1973. Long-range transmission of tree pollen to Shetland. II. Calculation of pollen deposition. *New Phytologist* 72, 183–190.
- van Hout, R., Chamecki, M., Brush, G., Katz, J., Parlange, M.B., 2008. The influence of local meteorological conditions on the circadian rhythm of corn (*Zea mays* L.) pollen emission. *Agricultural and Forest Meteorology* 148, 1078–1092.
- von Hase, A., Cowling, R.M., Ellis, A.G., 2006. Petal movement in cape wildflowers protects pollen from exposure to moisture. *Plant Ecology* 184, 75–87.
- von Wahl, P.-G., Puls, K.E., 1989. The emission of mugwort pollen (*Artemisia vulgaris* L.) and its flight in the air. *Aerobiologia* 5, 55–63.
- Waisel, Y., Eshel, A., Keynan, N., Langgut, D., 2008. *Ambrosia*: a new impending disaster for the Israeli allergic population. *Israel Medical Association Journal* 10, 856–857.
- Wang, S.Y., Spongberg, S.A., Rubenstein, J.S., 1985. Ragweed in China. *Nature* 316, 386.
- Weber, R.W., 2003. Meteorologic variables in aerobiology. *Immunology and Allergy Clinics of North America* 23, 411–422.
- Ziska, L.H., Caulfield, F.A., 2000. Rising CO₂ and pollen production of common ragweed (*Ambrosia artemisiifolia*), a known allergy-inducing species: implications for public health. *Australian Journal of Plant Physiology* 27, 893–898.